Total synthesis and biological characterization of SR-A3, a ternatin-related eEF1A inhibitor with enhanced cellular residence time

Hao-Yuan Wang[†], Keely Oltion[†], Amjad Ayad Qatran Al-Khdhairawi[§], Jean-Frédéric F. Weber[¶], and Jack Taunton[†,*]

[†]Department of Cellular and Molecular Pharmacology, University of California, San Francisco, CA 94158, United States

[§]School of Pharmacy, Faculty of Health & Medical Sciences, Taylor's University Lakeside Campus, 47500 Subang Jaya, Selangor, Malaysia

[¶]Atta-ur-Rahman Institute for Natural Product Discovery (AuRIns), Universiti Teknologi MARA (UiTM) Selangor Branch, 42300 Bandar Puncak Alam, Selangor, Malaysia

*corresponding author: jack.taunton@ucsf.edu

Abstract

Ternatin and related cyclic peptides inhibit the elongation phase of protein synthesis by targeting the eukaryotic elongation factor-1α (eEF1A), a potential therapeutic vulnerability in cancer and viral infections. The cyclic peptide natural product "A3" appears to be related to ternatin, but its complete structure is unknown and only 4 of its 11 stereocenters have been assigned. Hence, A3 could be any one of 128 possible stereoisomers. Guided by the stereochemistry of ternatin and more potent structural variants, we synthesized two A3 epimers, "SR-A3" and "SS-A3". We found that synthetic SR-A3 is indistinguishable from naturally derived A3 and potently inhibits cancer cell proliferation. Relative to SS-A3 and previously characterized ternatin variants, SR-A3 exhibits a dramatically enhanced duration of action. This increase in cellular residence time is conferred, stereospecifically, by a single β-hydroxy group attached to *N*-methyl leucine. SR-A3 thus exemplifies a mechanism for enhancing the pharmacological potency of cyclic peptide natural products via side-chain hydroxylation.

Introduction

Eukaryotic elongation factor-1α (eEF1A) is an essential component of the translation machinery.[1] During the elongation phase of protein synthesis, GTP-bound eEF1A delivers an aminoacyl-tRNA (aa-tRNA) to the ribosomal A site for selection. Base pairing between the A-site mRNA codon and aa-tRNA anticodon promotes GTP hydrolysis on eEF1A, releasing the aa-tRNA and facilitating peptide bond formation with the nascent peptidyl-tRNA in the P site. Because tumor cell growth and viral replication require elevated protein synthesis rates, eEF1A inhibitors – all of which are macrocyclic natural products – have been evaluated as potential anticancer and antiviral drugs.[2] Didemnin B,[3-4] cytotrienin A,[5] and nannocystin A[6] are examples of structurally diverse macrocycles that bind eEF1A and inhibit translation elongation. In 2019, dehydrodidemnin B (plitidepsin) was approved in Australia for the treatment of relapsed/refractory multiple myeloma.[7] Plitidepsin is currently being tested in hospitalized Covid-19 patients.

The natural product "A3" is a cyclic heptapeptide whose complete structure has not been reported. As described in a patent application, A3 was isolated from an Aspergillus strain and was found to inhibit cancer cell proliferation at low nanomolar concentrations.[8] Although its amino acid sequence and *N*-methylation pattern were elucidated, only 4 out of 11 stereocenters could be assigned (Figure 1). Motivated by its potent antiproliferative activity and unknown mechanism of action, we sought to determine which of the 128 possible stereoisomers (based on 7 unassigned stereocenters) corresponds to A3. Based on our hypothesis that A3 is structurally related to the anti-adipogenic cyclic heptapeptide, ternatin,[9] we previously designed and synthesized "ternatin-4", which incorporates the dehydromethyl leucine (dhML) and pipecolic acid residues found in A3, yet lacks the β-hydroxy group attached to *N*-Me-Leu (Figure 1). We discovered that ternatin and ternatin-4 inhibit cancer cell proliferation by targeting eEF1A, with ternatin-4 being up to 500-fold more potent than ternatin.[10] Recently, we found that

ternatin-4 potently blocks replication of the novel coronavirus SARS-CoV2, without obvious cytotoxic effects.[11]

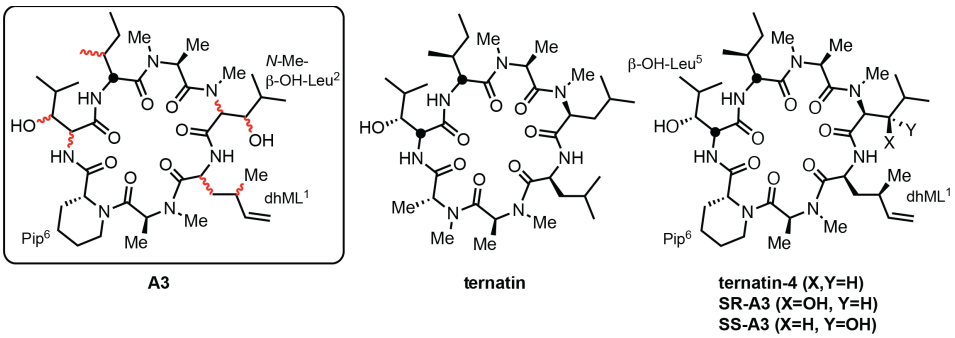

Figure 1. Partially determined structure of the natural product A3. Based on previous studies of ternatin and ternatin-4, we hypothesized that A3 corresponds to either one of two epimers, "SR-A3" or "SS-A3".

Although the potent antiproliferative activity exhibited by ternatin-4 suggested a structural kinship with naturally derived A3, this remained unproven. Assuming our structural hypothesis is correct, a single stereocenter in A3 (*N*-Me-β-OH-Leu side chain) remained ambiguous. A more intriguing question concerns the role of *N*-Me-β-OH-Leu in the biological activity of A3 as compared to ternatin and ternatin-4, both of which lack a β-hydroxy group at the equivalent position. Non-proteinogenic β-hydroxy amino acids are frequently found in macrocyclic natural products, yet the stereospecific roles of this biosynthetic modification are unknown in most cases. Here, we report the first total synthesis and biological characterization of two A3 epimers, SR-A3 and SS-A3, in which (*S,R*)- and (*S,S*)-*N*-Me-β-OH-Leu replaces *N*-Me-Leu of ternatin-4 (Figure 1). Synthetic SR-A3 is spectroscopically and biologically indistinguishable from the natural product A3, whereas SS-A3 has distinct properties. Similar to ternatin-4, SR-A3 potently inhibited cell proliferation and protein synthesis by targeting eEF1A. Transient exposure of cells to SR-A3, followed by washout, led to long-lasting inhibitory effects, whereas sustained inhibition was not observed with SS-A3 or ternatin-4. Our data thus reveal a striking and

stereospecific increase in cellular residence time conferred by a single oxygen atom appended to a macrocyclic eEF1A inhibitor.

Results and Discussion

Efficient synthesis of dehydromethyl leucine (dhML)

We previously found that replacing (*S*)-leucine in ternatin with (*S,R*)-dehydromethyl leucine (hereafter "dhML") leads to increased potency,[10] and we hypothesized that the stereochemistry of dhML in the natural product A3 is of the same configuration (Figure 1). Because our original 6-step synthesis of dhML methyl ester was low yielding and required a costly chiral auxiliary, we developed a more efficient, second-generation synthesis suitable for preparing gram quantities of Fmoc-dhML.

The copper(I)-promoted S_N2' reaction between a serine-derived organozinc reagent and allylic electrophiles has been previously exploited to synthesize amino acids that contain a γ-stereogenic center.[12-13] This method was appealing because it would provide dhML (as the Boc methyl ester) in only two steps from the inexpensive chiral building block, Boc-(*S*)-serine-OMe. Using previously reported conditions in which the organozinc reagent was generated in situ from Boc-iodoalanine-OMe **1**,[12] the S_N2' reaction with crotyl chloride **2** was slightly favored over the S_N2 pathway, providing the desired Boc-dhML-OMe **3** in 12% isolated yield (Figure 2, entry 1). After extensive optimization, aimed at improving S_N2' vs. S_N2 selectivity and conversion, we obtained Boc-dhML-OMe **3** in 43% isolated yield (1.6 g) through the use of 50 mol% CuBr·DMS and 2 equivalents of crotyl chloride (Figure 2, entry 8). When crotyl bromide was used, the S_N2 pathway became dominant (Figure 2, entry 7), indicating a key role of the leaving group in controlling pathway selectivity. The use of the CuBr·DMS complex was also critical, as other copper(I) salts, including CuBr, favored the S_N2 pathway or resulted in no reaction (Figure 2, entries 4-6). S_N2' diastereoselectivity is modest under the optimized reaction conditions, but the

desired product is easily purified by silica gel chromatography. Boc to Fmoc exchange, followed by ester hydrolysis, provided Fmoc-dhML **5** (Figure 2b), which was incorporated into the linear heptapeptide as described below.

a)

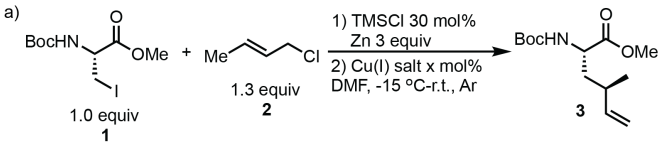

Entry	Cu(I) Salt	x	$S_N2':S_N2$ [a]	d.r. of S_N2' [a]	Yield [b]
1	CuBr·DMS	10	1.2:1	1:1	12%
2	CuBr·DMS	50	1.9:1	1.4:1	26%
3	CuBr·DMS	100	2.1:1	1.4:1	-
4	CuBr	100	1:3.5	-	-
5	CuCl	100	1:2.5	-	-
6	CuTC	100	-	-	N.R.
7[c]	CuBr·DMS	50	1:2.6	-	-
8[d]	**CuBr·DMS**	**50**	**1.8:1**	**1.4:1**	**43%**

[a] Ratio was based on the crude NMR of the reaction; [b] Isolated yield of **3**; [c] Crotyl bromide was used instead of **2**; [d] 2 equiv of crotyl chloride were used. DMS: dimethyl sulfide; TC: thiophene -2-carboxylate; N.R.: no reaction.

b)

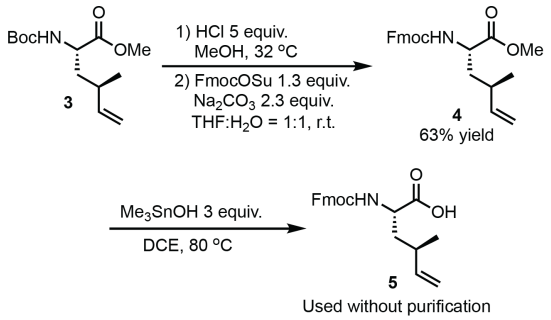

Figure 2. (a) Screening conditions to synthesize Boc-dhML-OMe **3** via Cu(I)-promoted S_N2' reaction. (b) Synthesis of Fmoc-dhML **5**.

Synthesis of ternatin-4, SS-A3, and SR-A3 via an improved macrocyclization strategy

A solid-phase route was previously employed to synthesize a linear heptapeptide precursor of ternatin, followed by solution-phase cyclization.[9] However, this strategy involved macrocyclization between the secondary amine of *N*-Me-Ala7 and the carboxylic acid of Leu1 (Figure 3a, site A), which we found to be low-yielding in the context of peptides containing dhML at the carboxy terminus.[10] Thus, we sought to identify an alternative cyclization site using the ternatin-related cyclic peptide **6** as a model system (Figure 3a). Linear heptapeptide precursors were synthesized on the solid phase, deprotected and cleaved from the resin, and cyclized in

solution (see Supporting Information for details). We failed to evaluate site B due to the poor resin loading of Fmoc-β-OH-Leu. Gratifyingly, cyclization at site C provided **6** in 63% overall yield (including the solid-phase linear heptapeptide synthesis), whereas cyclization at site A was less efficient (46% overall yield). By synthesizing the linear heptapeptide precursor on the solid phase and cyclizing in solution at site C, we were able to prepare ternatin-4 in 3 days and 70% overall yield (27 mg), a significant improvement over our previous route (Figure 3b). Most importantly, by incorporating Fmoc-protected (*S,R*)- and (*S,S*)-*N*-Me-β-OH-Leu, we completed the first total syntheses of SR-A3 (21 mg, 35% overall yield) and SS-A3 (5 mg, 21% overall yield).

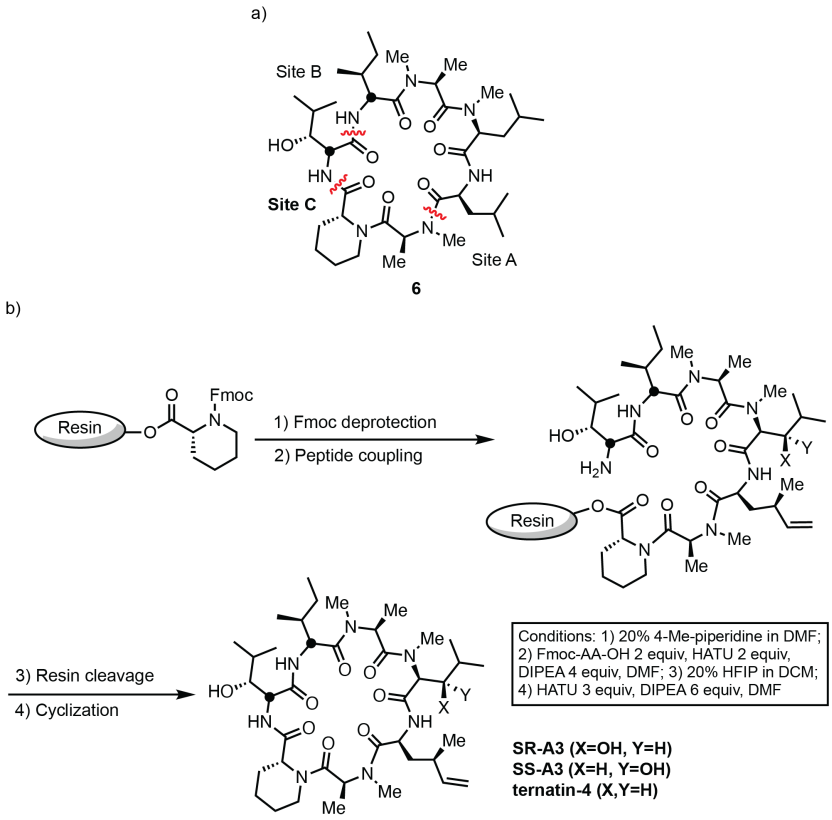

Figure 3. Solid-phase synthesis and macrocyclization strategy. (a) Identification of alternative cyclization sites. (b) Scheme for solid-phase synthesis of linear heptapeptide precursors, followed by solution-phase cyclization to provide ternatin-4, SR-A3, and SS-A3 (see Supporting Information for details).

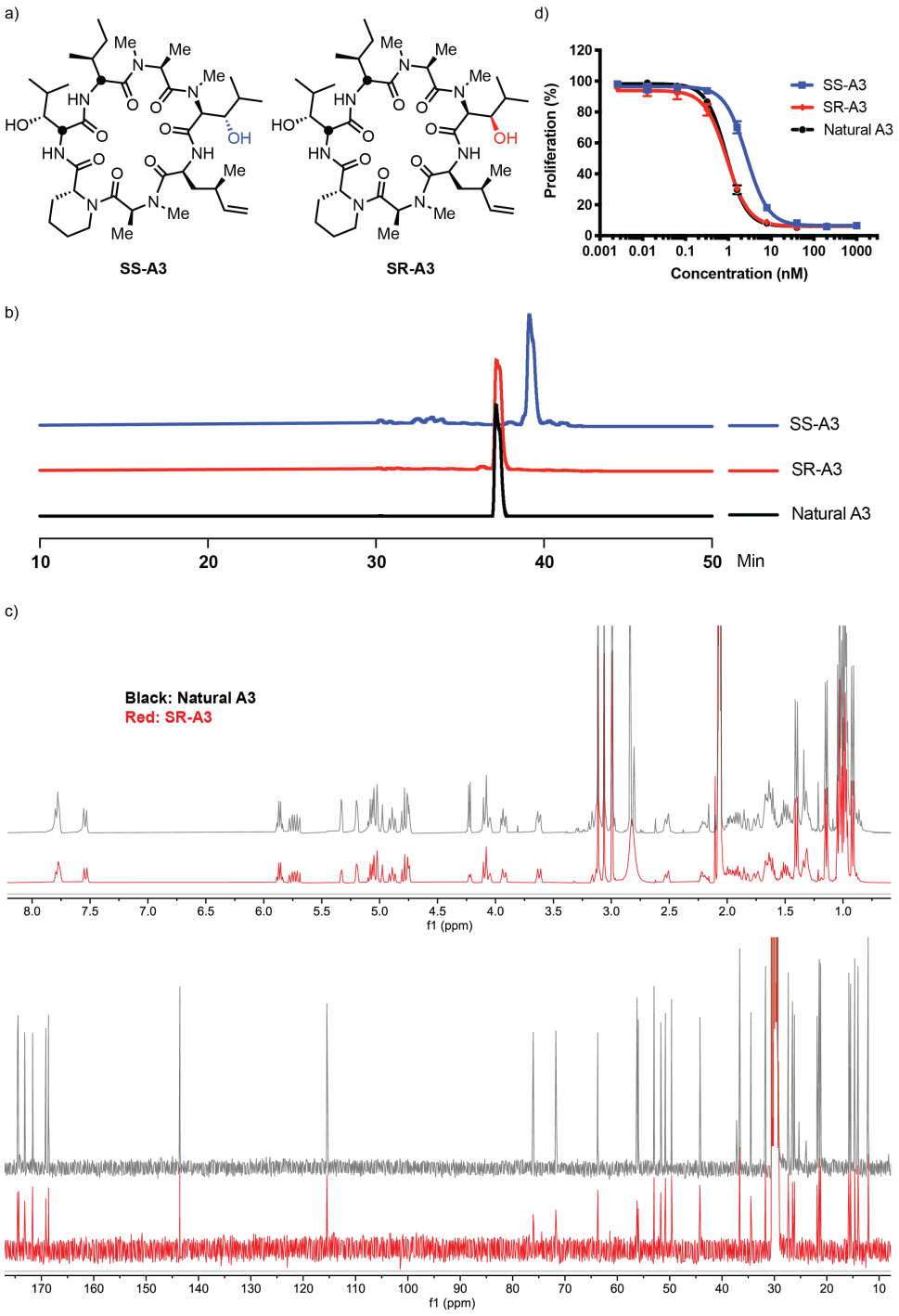

Figure 4. Comparison of naturally derived A3 with synthetic SS-A3 and SR-A3. a) Chemical structures of SS-A3 and SR-A3. b) HPLC elution profiles. c) Overlay of ^{1}H and ^{13}C NMR spectra in acetone-d_6. d) Concentration-dependent antiproliferative effects in HCT116 cells after 72 h.

Synthetic SR-A3 is indistinguishable from naturally derived A3

With synthetic SR-A3 and SS-A3 in hand (Figure 4a), we first compared their HPLC elution profiles with an authentic sample of the natural product A3. SR-A3 and naturally derived A3 had identical retention times, whereas SS-A3 eluted later in the gradient (Figure 4b). Furthermore, the H^1 and C^{13} NMR spectra of SR-A3 appeared identical to the corresponding spectra of natural A3 (Figure 4c). Finally, SR-A3 and naturally derived A3 blocked proliferation of HCT116 cancer cells with superimposable dose-response curves (Figure 4d, IC_{50} ~ 0.9 nM), whereas SS-A3 was ~3-fold less potent (IC_{50} ~2.7 nM). Together, these data are consistent with our stereochemical hypothesis and suggest that SR-A3 corresponds to the previously unknown structure of the natural product A3.

***N*-Me-β-OH-Leu stereospecifically confers increased cellular residence time**

We previously demonstrated that the antiproliferative effects of ternatin-4 were abrogated in cells expressing a point mutant of eEF1A (A399V).[10] Unsurprisingly, eEF1A-mutant cells were similarly resistant to SR-A3 (IC_{50} >> 1 μM), providing strong genetic evidence that eEF1A is a physiologically relevant target (Figure 5a). Consistent with this interpretation, treatment of cells with SR-A3 for 24 h reduced the rate of protein synthesis with an IC_{50} of ~20 nM (Figure 5b), as measured by a clickable puromycin incorporation assay (*O*-propargyl puromycin, OPP).[14] Under these conditions – 24 h of continuous treatment prior to a 1-h pulse with OPP – ternatin-4 behaved identically to SR-A3, whereas SS-A3 was slightly less potent. However, when the treatment time was shortened to 10 min before pulse-labeling with OPP for 1 h (in the continuous presence of the cyclic peptides), the dose-response curves shifted significantly, such that ternatin-4 was ~10-fold more potent than SR-A3 and SS-A3 had intermediate potency (Figure 5c). These data demonstrate: (1) replacing *N*-Me-Leu (ternatin-4) with *N*-Me-β-OH-Leu (SR-A3, SS-A3) results in *decreased* potency (or no significant difference) under continuous

exposure conditions, and (2) the relative potency of SR-A3, SS-A3, and ternatin-4 is time-dependent. The latter effect is likely due to intrinsic differences in cell permeability and/or eEF1A binding kinetics.

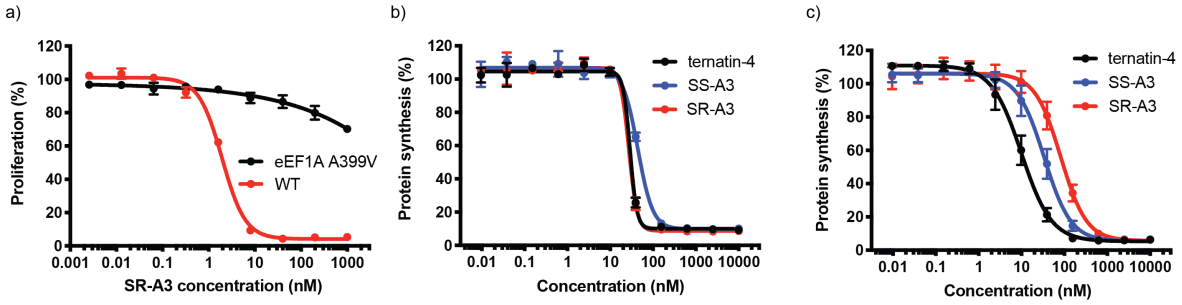

Figure 5. SR-A3 inhibits protein synthesis via eEF1A and exhibits a time-dependent potency shift. a) Wild-type and eEF1A-mutant (A399V) HCT116 cells were treated with SR-A3 for 72 h. Cell proliferation (% DMSO control) was quantified using AlamarBlue. b) and c) HCT116 cells were treated with the indicated compounds for 24 h or 10 min, respectively, and protein synthesis (% DMSO control) was quantified after pulse labeling with *O*-propargyl puromycin for 1 h (see Supporting Information). Data points (% DMSO control) are mean values ± SD (n = 3).

Drug-target residence time, which reflects not only the intrinsic biochemical off-rate, but also the rebinding rate and local target density in vivo, has emerged as a critical kinetic parameter in drug discovery.[15-16] To test for potential differences in cellular residence time, we treated HCT116 cells with 100 nM SR-A3, SS-A3, or ternatin-4 for 4 h, followed by washout into compound-free media. At various times post-washout, cells were pulse-labeled with OPP for 1 h. Whereas protein synthesis rates partially recovered in cells treated with ternatin-4 or SS-A3 (~30% of DMSO control levels, 24 h post-washout), transient exposure of cells to SR-A3 resulted in sustained inhibition (Figure 6a). To confirm the extended duration of action observed with SR-A3, we assessed cell proliferation during a 72-h washout period. Strikingly, cell proliferation was nearly abolished after 4-h treatment with 100 nM SR-A3, followed by rigorous washout. By contrast, cell proliferation rates recovered to ~50% of DMSO control levels after transient exposure to 100 nM ternatin-4 or SS-A3. These results demonstrate that the (*R*)-β-

hydroxy group attached to *N*-Me-Leu endows SR-A3 with a kinetic advantage over SS-A3 and ternatin-4, as reflected by washout resistance and increased cellular residence time.

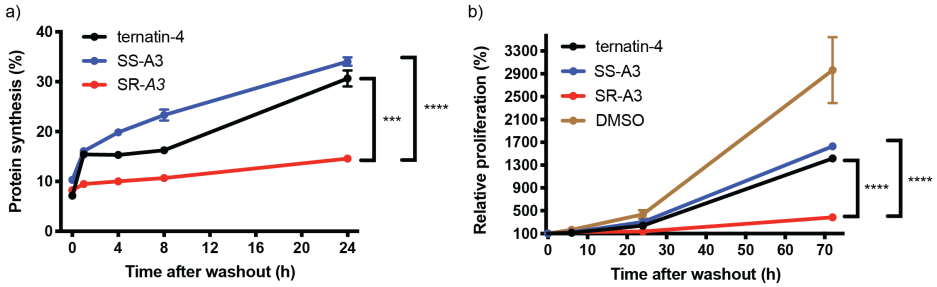

Figure 6. *N*-Me-β-OH-Leu stereospecifically endows SR-A3 with increased cellular residence time. a) HCT116 cells were treated with the indicated compounds (100 nM) or DMSO for 4 h, followed by rigorous washout into compound-free media. At the indicated time points post-washout, cells were pulse-labeled with OPP (1 h), and OPP incorporation was quantified. Normalized data (% DMSO control) are mean values ± SD (n = 3). b) HCT116 cells were treated with the indicated compounds (100 nM) or DMSO for 4 h, followed by rigorous washout into compound-free media. At the indicated time points post-washout, cell proliferation was quantified using the CellTiter-Glo assay. Normalized data (% DMSO control at t = 0 h post-washout) are mean values ± SD (n = 3). ***, P < 0.001; ****, P < 0.0001.

Conclusions and Perspective

In this study, we developed an improved synthetic route to dhML-containing ternatin variants, culminating in the total synthesis of SR-A3 and SS-A3. Our work provides spectroscopic, chromatographic, and pharmacological evidence that synthetic SR-A3 (and not SS-A3) is identical to the natural product "A3". An unexpected finding from our experiments with cancer cell lines is that the β-hydroxy group in SR-A3 does not confer increased potency under continuous treatment conditions. Rather, SR-A3 exhibits a dramatic increase in cellular residence time, as revealed by washout experiments followed by assessment of protein synthesis and cell proliferation rates. SR-A3 thus provides a compelling illustration of how a "ligand efficient" side-chain modification can be exploited to alter the pharmacological properties of a cyclic peptide natural product.

Acknowledgments

Funding for this study was provided by the UCSF Program for Breakthrough Biomedical Research (JT) and the Tobacco-Related Disease Research Program Postdoctoral Fellowship Awards (28FT-0014 to HW). Part of this work was supported by Taylor's University PhD Scholarship program (AAQAK), as well as a research grant from the Ministry of Education of Malaysia FRGS [600-IRMI/FRGS 5/3 (011/2017) to JFW]. UCSF has filed a provisional patent application based on part of this work; JT, HW, and KO are listed as inventors.

References

1. Schuller, A. P.; Green, R., Roadblocks and resolutions in eukaryotic translation. *Nat Rev Mol Cell Biol* **2018,** *19* (8), 526-541.
2. Abbas, W.; Kumar, A.; Herbein, G., The eEF1A Proteins: At the Crossroads of Oncogenesis, Apoptosis, and Viral Infections. *Front Oncol* **2015,** *5*, 75.
3. Crews, C. M.; Collins, J. L.; Lane, W. S.; Snapper, M. L.; Schreiber, S. L., GTP-dependent binding of the antiproliferative agent didemnin to elongation factor 1 alpha. *J. Biol. Chem.* **1994,** *269* (22), 15411-15414.
4. Shao, S.; Murray, J.; Brown, A.; Taunton, J.; Ramakrishnan, V.; Hegde, R. S., Decoding Mammalian Ribosome-mRNA States by Translational GTPase Complexes. *Cell* **2016,** *167* (5), 1229-1240 e1215.
5. Lindqvist, L.; Robert, F.; Merrick, W.; Kakeya, H.; Fraser, C.; Osada, H.; Pelletier, J., Inhibition of translation by cytotrienin A--a member of the ansamycin family. *RNA* **2010,** *16* (12), 2404-2413.
6. Krastel, P.; Roggo, S.; Schirle, M.; Ross, N. T.; Perruccio, F.; Aspesi, P., Jr.; Aust, T.; Buntin, K.; Estoppey, D.; Liechty, B., et al., Nannocystin A: an Elongation Factor 1 Inhibitor from Myxobacteria with Differential Anti-Cancer Properties. *Angew. Chem. Int. Ed.* **2015,** *54* (35), 10149-10154.
7. Spicka, I.; Ocio, E. M.; Oakervee, H. E.; Greil, R.; Banh, R. H.; Huang, S. Y.; D'Rozario, J. M.; Dimopoulos, M. A.; Martinez, S.; Extremera, S., et al., Randomized phase III study (ADMYRE) of plitidepsin in combination with dexamethasone vs. dexamethasone alone in patients with relapsed/refractory multiple myeloma. *Ann Hematol* **2019,** *98* (9), 2139-2150.
8. Blunt, J.; Cole, T.; Munro, M.; Sun, L.; Weber, J.-F. R.; Ramasamy, K.; Bakar, H. A.; Majeed, A. B. B. A., Bioactive compounds. *International Patent WO 2010/062159 A1*.
9. Shimokawa, K.; Mashima, I.; Asai, A.; Yamada, K.; Kita, M.; Uemura, D., (−)-Ternatin, a highly N-methylated cyclic heptapeptide that inhibits fat accumulation: structure and synthesis. *Tetrahedron Lett.* **2006,** *47* (26), 4445-4448.
10. Carelli, J. D.; Sethofer, S. G.; Smith, G. A.; Miller, H. R.; Simard, J. L.; Merrick, W. C.; Jain, R. K.; Ross, N. T.; Taunton, J., Ternatin and improved synthetic variants kill cancer cells by targeting the elongation factor-1A ternary complex. *Elife* **2015,** *4:e10222*.
11. Gordon, D. E.; Jang, G. M.; Bouhaddou, M.; Xu, J.; Obernier, K.; White, K. M.; O'Meara, M. J.; Rezelj, V. V.; Guo, J. Z.; Swaney, D. L., et al., A SARS-CoV-2 protein interaction map reveals targets for drug repurposing. *Nature* **2020,** *583* (7816), 459-468.
12. Deboves, H. J. C.; Grabowska, U.; Rizzo, A.; Jackson, R. F. W., A new route to hydrophobic amino acids using copper-promoted reactions of serine-derived organozinc reagents. *Journal of the Chemical Society-Perkin Transactions 1* **2000,** (24), 4284-4292.
13. Dunn, M. J.; Jackson, R. F. W.; Pietruszka, J.; Turner, D., Synthesis of Enantiomerically Pure Unsaturated .alpha.-Amino Acids Using Serine-Derived Zinc/Copper Reagents. *The Journal of Organic Chemistry* **1995,** *60* (7), 2210-2215.
14. Liu, J.; Xu, Y.; Stoleru, D.; Salic, A., Imaging protein synthesis in cells and tissues with an alkyne analog of puromycin. *Proc. Natl. Acad. Sci. U.S.A.* **2012,** *109* (2), 413-418.
15. Vauquelin, G., Rebinding: or why drugs may act longer in vivo than expected from their in vitro target residence time. *Expert Opin Drug Discov* **2010,** *5* (10), 927-941.
16. Copeland, R. A., The drug-target residence time model: a 10-year retrospective. *Nat Rev Drug Discov* **2016,** *15* (2), 87-95.